JOC The Journal of Organic Chemistry

Article

pubs.acs.org/joc

Origins of Stereoselectivity of Chiral Vicinal Diamine-Catalyzed Aldol Reactions

Adam Simon, Alexander J. Yeh, Yu-hong Lam, and K. N. Houk*

Department of Chemistry and Biochemistry, University of California, Los Angeles, 607 Charles E. Young Drive East, Los Angeles, California 90095-1569, United States

Supporting Information

ABSTRACT: The sources of asymmetric induction in aldol reactions catalyzed by cinchona alkaloid-derived amines, and chiral vicinal diamines in general, have been determined by density functional theory calculations. Four vicinal diamine-catalyzed aldol reactions were examined. The cyclic transition states of these reactions involve nine-membered hydrogen-bonded rings in distinct conformations. Using nomenclature from eight-membered cycloalkanes, the heavy atoms of the low-energy transition states are in crown (chair−chair) and chair-boat conformations. The factors that control which of these are favored have been identified.

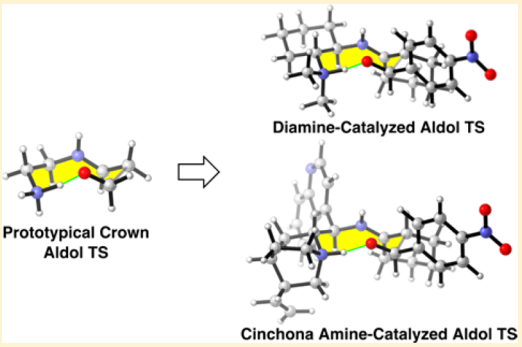

INTRODUCTION

The functionalization of carbonyl compounds by asymmetric aminocatalysis has proven to have considerable synthetic utility.[1] Proline and its derivatives are widely used chiral amines for enantioselective reactions.[2] The collaborations of experimentalists and computational chemists have revealed the mechanistic intricacies of asymmetric aldol reactions catalyzed by proline.[3] Vicinal diamines are another general class of related catalysts and are alternatives to proline.[4]

Both vicinal diamines and proline rely on enamine and iminium chemistry. Proline has a carboxylic acid while one of the amines of a diamine can be protonated and function as a general acid. These catalysts vary from simple 1,2-diaminocyclohexanes (**3**) to more complex cinchona alkaloid-derived amines **1** and **2** (Scheme 1). The vicinal diamines, **3** and **4**, are important catalysts for aldol reactions. A summary of aldol reactions involving chiral vicinal diamine catalysts is shown in Scheme 2. Yamamoto, using diamine **4**, reported one of the first examples of vicinal diamine-catalyzed aldol reactions (Scheme 2, eq 1).[4] They used acetone, as well as cyclic ketones, with *p*-nitrobenzaldehyde as the aldol acceptor and reported good to excellent enantioselectivity. Luo reported a successful and robust series of aldol reactions catalyzed by **3** (Scheme 2, eq 2).[5] Catalyst **3** works with linear aliphatic ketone donors with excellent stereocontrol, and gives unprecedented *syn* diastereoselectivity for ethyl ketones.[5]

The cinchona alkaloid-derived primary amine catalysts **1** and **2** are pseudoenantiomers because the important stereogenic centers at C8 and C9 are inverted. These cinchona alkaloid-derived primary amines have been studied spectroscopically and computationally.[6−8] While **1** and **2** are conformationally flexible, both the ground state and transition states of the reactions that they catalyze have a common conformational preference.[7−9]

Scheme 1. Examples of Vicinal Diamines

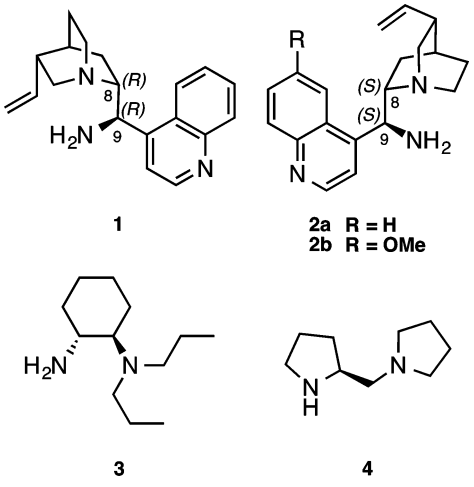

The use of cinchona-derived amine catalysts both complemented and expanded the synthetic utility of chiral pyrrolidine-based secondary amines in aldol chemistry.[10−13] Cinchona alkaloid-derived primary amines are advantageous over secondary amine catalysts for reactions involving sterically demanding functional groups.[14] The first example of asymmetric intermolecular aldol reactions catalyzed by cinchonine- and cinchonidine-based primary amines (**1** and **2a**) was reported in 2007 (Scheme 2, eq 3).[10] Later, these catalysts,

Received: October 19, 2016
Published: November 14, 2016

DOI: 10.1021/acs.joc.6b02542
J. Org. Chem. 2016, 81, 12408−12415

Scheme 2. Examples of Aldol Reactions Catalyzed by Chiral Vicinal Diamines

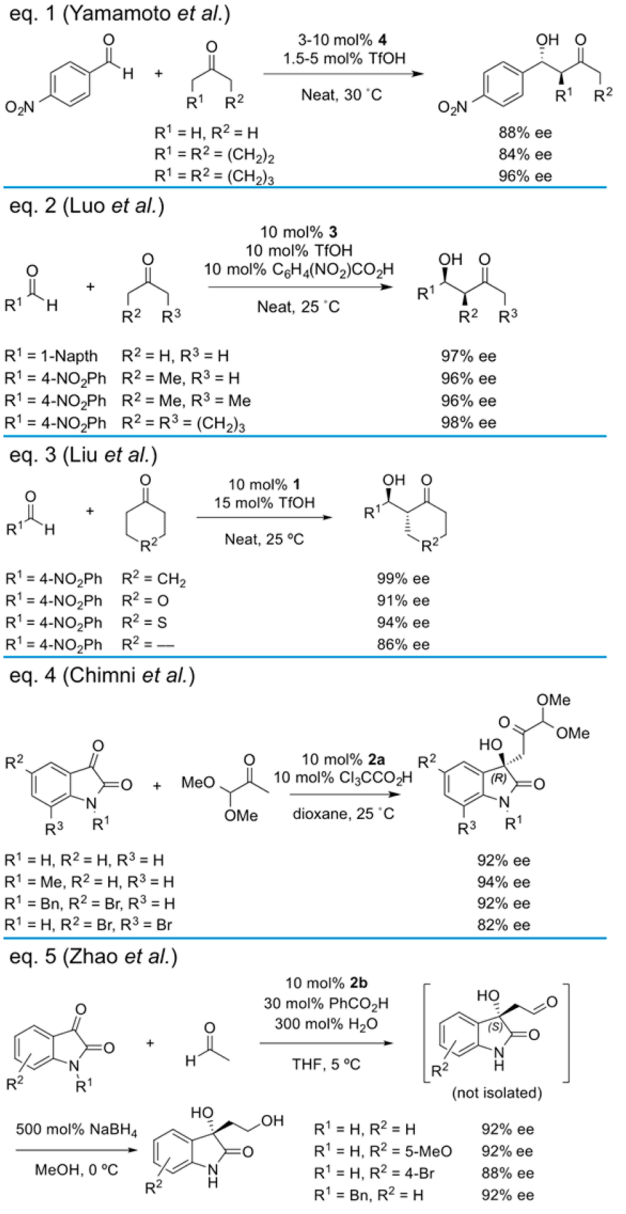

including quinine-derived primary amines (**2b**), were shown to perform well with more complex substrates, which sometimes reacted overly slow with secondary amine-based catalysts (Scheme 2, eq 4−5).[12,13]

The sources of asymmetric induction in the reactions by Liu,[10] Chimni,[13] and Zhao[12] (Scheme 2, eq 3−5) are not well-known, and they have mostly been explained by *ad hoc* models in the original reports. The origins of asymmetric induction of vicinal diamine-catalyzed aldol reactions were only recently explored by our group[9,15] and the Zhang group.[16] Our efforts have shown that the stereoselectivities of intra- and intermolecular aldol reactions are determined by favored conformations of cyclic transition states.[9,15]

We now present quantum chemical calculations of transition states for the more complex examples of these reactions reported by Liu,[10] Chimni,[13] and Zhao[12] in Scheme 2. The privileged cinchona alkaloid-derived primary amines are examined with classical substrates, i.e., cyclohexanone and *p*-nitrobenzaldehyde, and pharmaceutically relevant isatin-based substrates. Additionally, we revisit computations by the Zhang group[16] for the sources of stereoselectivity in the aldol reactions reported by Luo (Scheme 2, eq 2).[5] A general method to explain the source of asymmetric induction in vicinal diamine-catalyzed reactions is proposed.

COMPUTATIONAL METHODS

All quantum chemical calculations were performed with Gaussian 09.[17] Geometry optimizations and frequencies were calculated with the B3LYP[18] density functional with the 6-31G(d) basis set in conjunction with the IEF-PCM implicit solvation model.[19] Optimized geometries were verified by frequency calculations as minima (zero imaginary frequencies) or transition structures (a single imaginary frequency). Free energy corrections were calculated using Truhlar's quasiharmonic approximation.[20] Single point energy calculations were performed on optimized geometries with the M06-2X[21] density functional and def2-TZVPP[22] basis set with the IEF-PCM model for the experimental solvent reported. The thermal corrections evaluated from the unscaled vibrational frequencies at the B3LYP/6-31G(d)-IEF-PCM level on the optimized geometries were then added to the M06-2X/def2-TZVPP−IEF-PCM electronic energies to obtain the free energies. We previously tested how several density functionals perform with the model system[15] and found that the M06-2X/def2-TZVPP-IEF-PCM//B3LYP/6-31G(d)-IEF-PCM provided accurate energies while being relatively efficient in terms of computational times.[23] B3LYP/6-31G(d) provides appropriate geometry structures, but dispersion-inclusive methods with larger basis sets are required for accurate energies.[9a]

Monte Carlo conformational searches were performed on the enamines formed by the protonated catalysts and aldol donors in the presence of the aldol acceptors to identify reactive conformations with the OPLS_2005 force field[24] in Maestro/Macromodel.[25] Reactive conformations with the distance between the bond-forming atoms shorter than 4.0 Å were used as input geometries for transition structure optimizations. Structure graphics were generated using CYLView.[26]

RESULTS AND DISCUSSION

We previously studied the origins of stereoselectivity in intramolecular aldol condensations catalyzed by cinchona alkaloid-derived primary amine **2b**.[9a,11,27] The stereochemistry-determining transition structures by Lam and Houk are shown in Scheme 3. These reactions proceed through a nine-membered hydrogen bonded cyclic transition state, where the eight heavy atoms adopt conformations that resemble low-energy conformations of cyclooctane.[28] The lowest-energy transition structure adopts the boat-chair conformation, and leads to the major enantiomer. The minor product was predicted to form via the cyclic transition structure in the crown conformation.

The transition states of intermolecular aldol reactions catalyzed by the parent vicinal diamine were also reported in an earlier communication.[15] The prototypical vicinal diamine-catalyzed aldol transition structures (Scheme 4) display well-defined conformations, with a preference for the crown conformation. Chair conformations about the forming C−C bonds were found in the low-energy crown and chair-boat conformations. The s-trans enamines (crown and chair-boat) were found to be preferred over s-cis enamines (boat-chair and boat−boat). We also explained Yamamoto's vicinal diamine-catalyzed aldol reaction shown in Scheme 5.[4] The crown with an equatorial aryl substituent formed the observed major product, while the crown with an axial aryl substituent formed

DOI: 10.1021/acs.joc.6b02542
J. Org. Chem. 2016, 81, 12408−12415

Scheme 3. Stereo-Determining Transition Structures by Lam and Houk[9a]

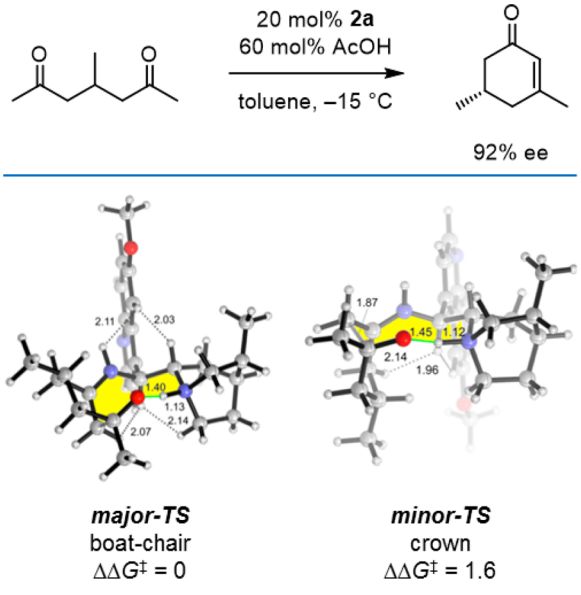

Scheme 4. Prototypical Vicinal-Diamine Catalyzed Aldol Transition Structures[15]

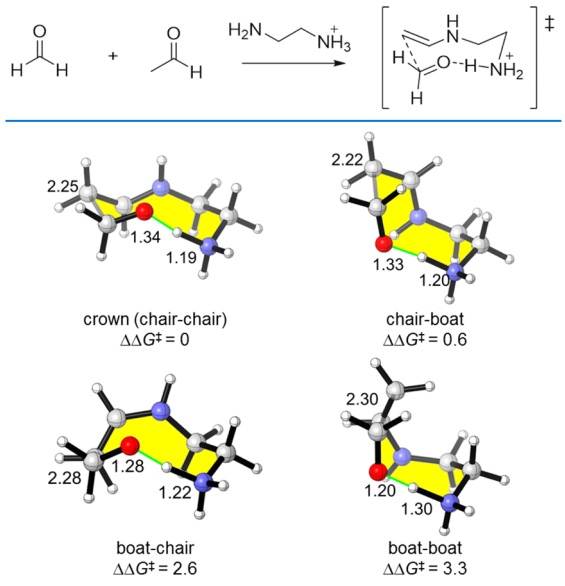

the minor enantiomeric product, reminiscent of the Zimmerman−Traxler model.[29]

In 2007, Liu reported that the aldol reactions of cyclohexanones and substituted benzaldehydes were effectively catalyzed by the cinchona alkaloid-derived vicinal diamine **1** (Scheme 6).[10] They observed 99% ee, with a diastereomeric ratio of 9.2:1 for the example in Scheme 6. This corresponds to a difference in free energies of activation ($\Delta\Delta G^{\ddagger}$) of ≥2.9 kcal/mol for enantioselectivity and 1.2 kcal/mol for diastereoselectivity.

Four transition structures for the aldol reaction of *p*-nitrobenzaldehyde and the enamine formed by **1** and cyclohexanone were located (Figure 1). As reported earlier,[15] the transition structures are nine-membered hydrogen-bonded rings that have heavy atoms resembling conformations of cyclooctane.[28] The quinoline ring is equatorial in the favored

Scheme 5. Stereo-Determining Transition Structures for Yamamoto's Aldol Reaction[15]

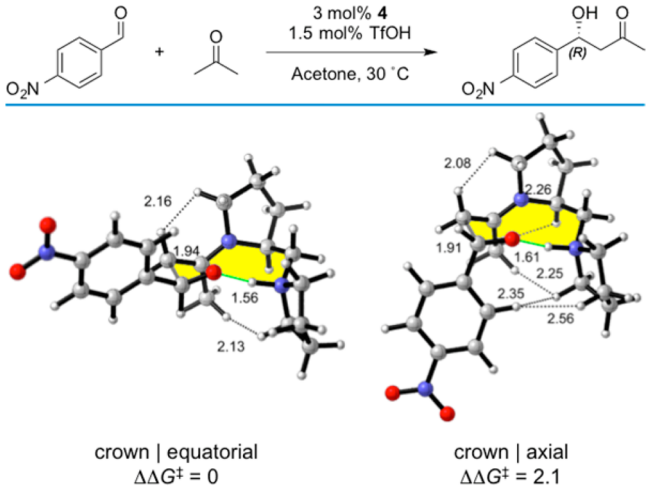

Scheme 6. Example Aldol Reaction Reported by Liu

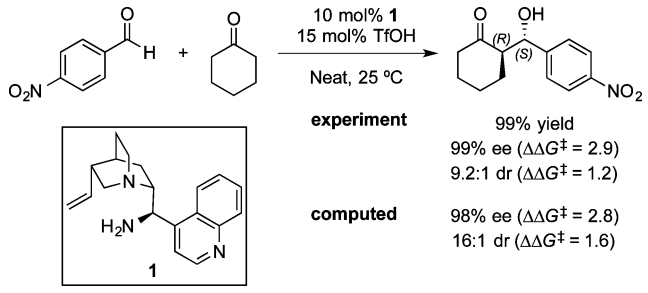

transition structures. Additional higher-energy stereoisomeric transition structures are shown in Figure S3 and S4.

TS-1a leads to the major (*R*,*S*) *anti*-product and is the lowest-energy transition structure. The (*R*,*R*) *syn*-diastereomer is formed from **TS-1b** and is higher in energy by 1.6 kcal/mol compared with **TS-1a**. Both **TS-1a** and **TS-1b** are crown conformations, have staggered conformations about the forming C−C bond, and have s-trans enamine conformations of the catalyst. These two transition structures differ by the equatorial and axial nature of the *p*-nitrobenzaldehyde group. **TS-1c** also leads to a *syn*-diastereomer, but with the (*S*,*S*) absolute configuration. This transition structure is higher in energy by 2.8 kcal/mol. **TS-1c** is in a boat-chair conformation, and contains a steric interaction between the s-cis enamine and the quinoline ring of the catalyst. The proximal H···H interaction is at 2.73 Å. The forming C−C bond is rather eclipsed with a dihedral angle of 36° at the OC−CC bond. The absolute configuration of the minor diastereomer has not been reported,[10] but we predict that the (*R*,*R*) *syn*-product is preferred via **TS-1b**, in close agreement with experimental diastereoselectivity.

The minor (*S*,*R*) enantiomer is formed by **TS-1d**, which is higher in energy than **TS-1a** by 2.8 kcal/mol, also in close agreement with experimental enantioselectivity. **TS-1d** is in the chair-boat conformation, which has a staggered arrangement at the forming C−C bond between the s-trans enamine and electrophilic carbonyl carbon. **TS-1d** contains steric interactions between the axial alkyl group of the enamine and the quinoline ring of the catalyst. These H···H interactions in the chair-boat are 2.44 and 2.53 Å. Thus, the destabilization of the

DOI: 10.1021/acs.joc.6b02542
J. Org. Chem. 2016, 81, 12408−12415

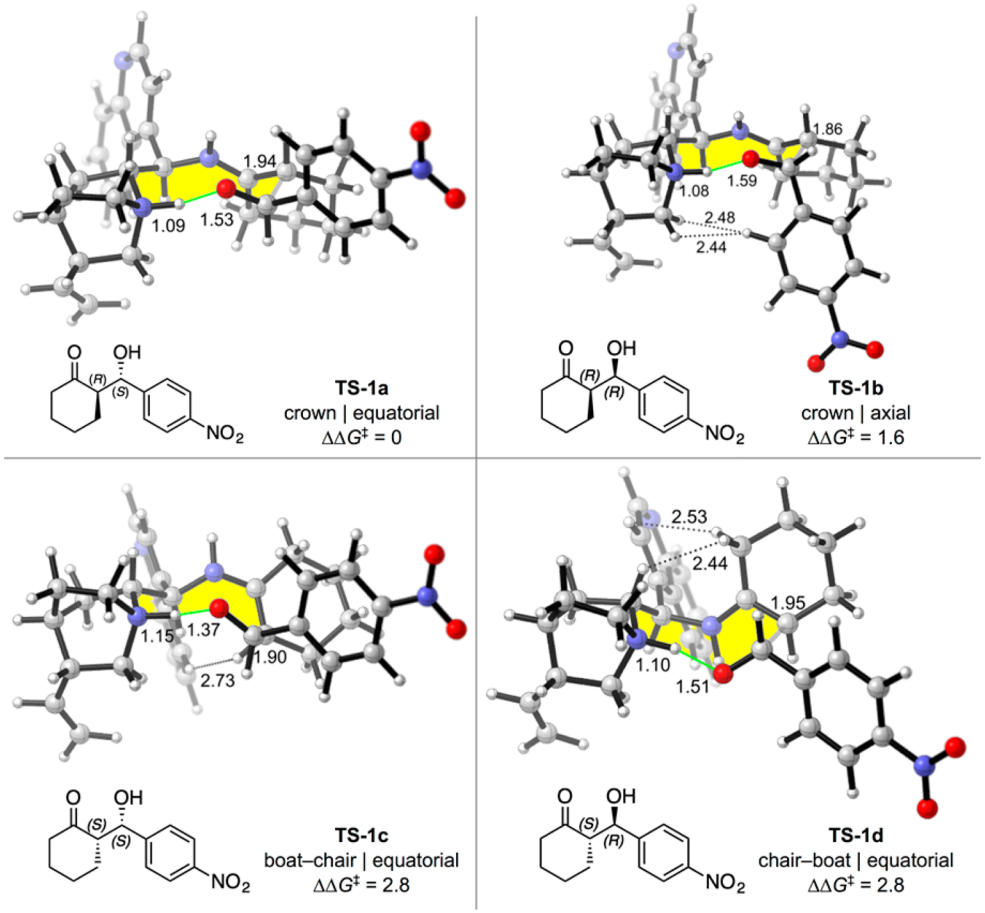

Figure 1. Lowest-energy transition structures **TS-1a–d** for the aldol addition of *p*-nitrobenzaldehyde and the enamine formed by **1** and cyclohexanone (M06-2X/def2-TZVPP-IEF-PCM//B3LYP/6-31G(d)-IEF-PCM (cyclohexanone)). The free energies of activation ($\Delta\Delta G^{\ddagger}$), relative to **TS-1a**, are reported in kcal/mol.

chair-boat results from steric repulsions between the axial methylene of the cyclohexanone and the quinoline ring of the catalyst.

We also studied the aldol reactions reported by Chimni[13] and Zhao[12] to explore how complex substrates affected the conformational preferences of the aldol transition state (Scheme 7). Catalysts **2a** and **2b** possess the same absolute configuration at C8 and C9, yet the senses of stereoselectivity of the two reactions are opposite. The (*R*) product reported by Chimni is formed from the addition to the *Si* face of isatin by the enamine derived from **2a** and pyruvic aldehyde dimethyl acetal in 92% ee ($\Delta\Delta G^{\ddagger}$ = 1.9 kcal/mol). The reaction reported by Zhao, however, yields the (*S*) product requiring *Re* selectivity at the isatin by the enamine derived from **2b** and acetaldehyde also in 92% ee ($\Delta\Delta G^{\ddagger}$ = 1.8 kcal/mol).

For Chimni's aldol reaction (Scheme 7, eq 1), the two lowest-energy stereocontrolling transition structures are shown in Figure 2. Higher-energy stereoisomeric transition structures are shown in Figure S5. **TS-2a** leads to the major (*R*) product and is the lowest-energy transition structure. The minor (*S*) enantiomer forms from **TS-2b**. The difference in free energy of activation ($\Delta\Delta G^{\ddagger}$) between **TS-2a** and **TS-2b** is 3.6 kcal/mol, which overestimates the reported enantioselectivity.

TS-2a and **TS-2b** have similar conformations at the cinchona alkaloid-derived primary amine catalyst. Both enamines are s-trans and the quinoline rings are equatorial. The chair-boat is destabilized by a steric clash between the axial dimethoxymethyl group of the enamine and quinoline ring of the catalyst. The major H···H interactions are 2.50 and 2.40 Å between the axial CH of the enamine, quinoline ring, and C8–H of the catalyst.

The two lowest-energy transition structures for Zhao's aldol reaction (Scheme 7, eq 2) are shown in Figure 3.

Scheme 7. Aldol Reactions Reported by Chimni and Zhao

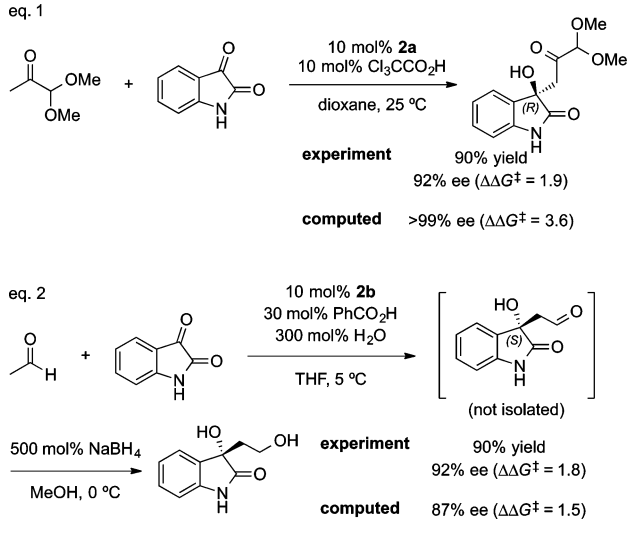

DOI: 10.1021/acs.joc.6b02542
J. Org. Chem. 2016, 81, 12408–12415

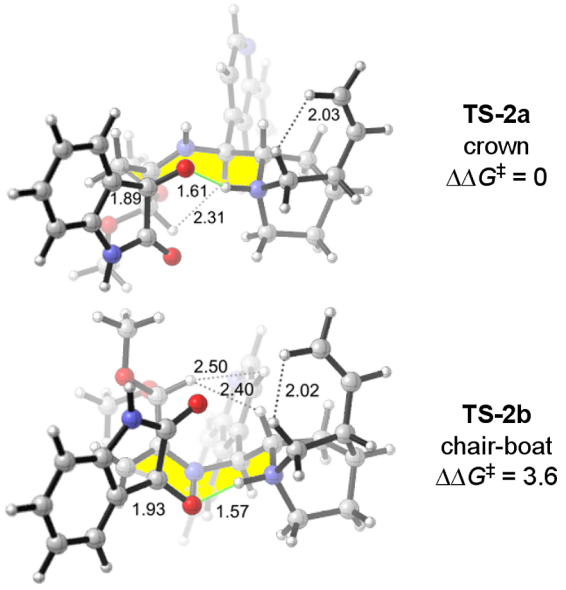

Figure 2. Lowest-energy transition structures **TS-2a** and **TS-2b** for the aldol addition of isatin and the enamine formed by **2a** and pyruvic aldehyde dimethyl acetal (M06-2X/def2-TZVPP-IEF-PCM//B3LYP/6-31G(d)-IEF-PCM (1,4-dioxane)). The free energies of activation ($\Delta\Delta G^{\ddagger}$), relative to **TS-2a**, are reported in kcal/mol.

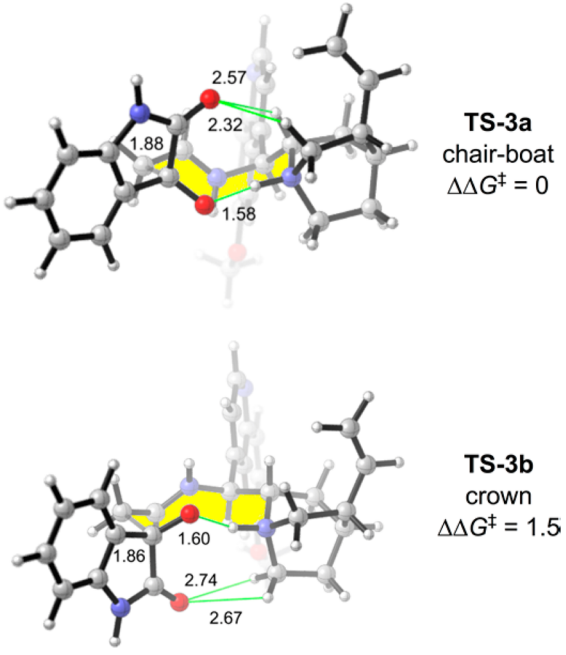

Figure 3. Lowest-energy transition structures **TS-3a** and **TS-3b** for the aldol addition of isatin and the enamine formed by **2b** and acetaldehyde (M06-2X/def2-TZVPP-IEF-PCM//B3LYP/6-31G(d)-IEF-PCM (THF)). The free energies of activation ($\Delta\Delta G^{\ddagger}$), relative to **TS-3a**, are reported in kcal/mol.

Higher-energy stereoisomeric transition structures are displayed in Figure S7. **TS-3a**, the favored transition structure, is in the chair-boat conformation, with an s-trans enamine and equatorial quinoline ring. With an aldehyde aldol donor, there is no steric interaction between the axial substituent of the enamine and quinoline ring in the chair-boat. **TS-3b** is in the crown conformation with both an s-trans enamine and equatorial quinoline ring. We found that the distances between the amide carbonyl oxygen and the polarized CH's adjacent to the protonated quinuclidinium nitrogen are quite close in both **TS-3a** and **TS-3b**.

In **TS-3a** there are two $^{+}$NCH···O$^{\delta-}$ interactions at 2.57 and 2.32 Å. In the crown, **TS-3b**, these are further apart at 2.74 and 2.67 Å. Thus, there are hydrogen-bonding interactions between the amide carbonyl oxygen and the polarized alkyl groups adjacent to the quinuclidinium nitrogen, which are stronger in the chair-boat conformation. Electrostatic $^{+}$NCH···O$^{\delta-}$ interactions are also present in the Houk-List model for proline-catalyzed aldol additions.[3a]

To test the importance of this electrostatic interaction, we computed a model of the reaction, where the amide functional group in the aldol transition structures **TS-4a** and **TS-4b** is replaced with methylene groups. The crown and chair-boat conformations with the model reactant are shown in Figure 4.

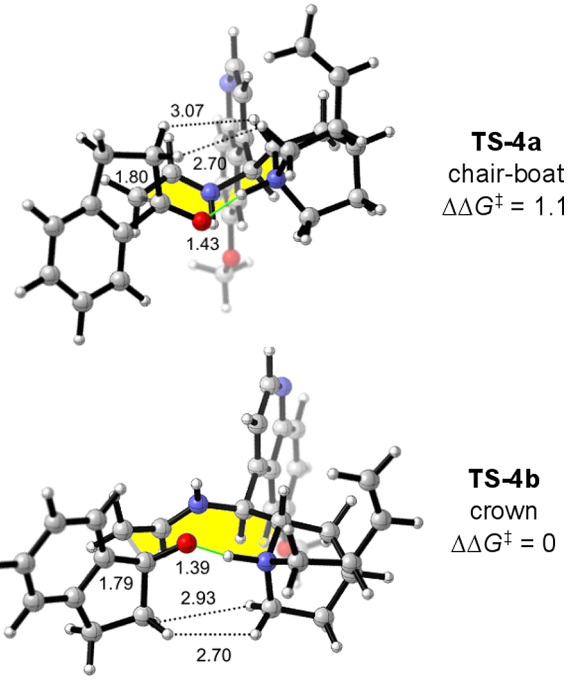

Figure 4. Model aldol system where the amide functional group of isatin was replaced with methylenes. The transition structures **TS-4a** and **TS-4b** are modified structures from **TS-3a** and **TS-3b**, which were calculated at the M06-2X/def2-TZVPP-IEF-PCM//B3LYP/6-31G(d)-IEF-PCM (THF) level of theory. The free energies of activation ($\Delta\Delta G^{\ddagger}$), relative to **TS-4b**, are reported in kcal/mol.

TS-4a, the chair-boat, is higher in energy than **TS-4b**, the crown, by 1.1 kcal/mol. Thus, hydrogen bonding between the amide carbonyl oxygen and polarized alkyl groups overcome the intrinsic conformational preferences of the aldol transition state in Zhao's aldol reaction with aldehyde aldol donors. These results explain the difference in facial selectivities of the enamine additions to isatin in the reactions reported by Chimni[13] and Zhao.[12]

Luo reported a robust methodology for bimolecular aldol reactions catalyzed by the vicinal diamine **3**.[5a] One example, similar to the reaction reported by Liu[10] in the same year, is the aldol addition of *p*-nitrobenzaldehyde and cyclohexanone catalyzed by **3** (Scheme 8). The reaction achieved 98% ee with 9:1 dr, corresponding to difference in free energies of activation of 2.7 and 1.2 kcal/mol, respectively.

DOI: 10.1021/acs.joc.6b02542
J. Org. Chem. 2016, 81, 12408−12415

Scheme 8. Example Aldol Reaction Reported by Luo

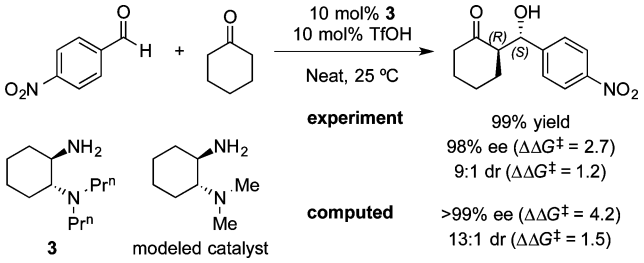

In 2012, the Zhang group reported computational studies of three aldol reactions reported by Luo, including the reaction in Scheme 8.[16] They calculated the transition structures for the reactions at the B3LYP/6-311+G(d,p)//B3LYP/6-31G(d) level of theory and explained the reported enantioselectivities and diastereoselectivities. Their chemical analysis involves the conformations of the enamines and using Newman projections down the forming C−C bond, reminiscent of the Houk-List model. The differences in energy between the stereoisomeric transition structures were rationalized by the degree of planarity of the enamine and dihedral angle of the forming C−C bonds. The model proposed by the Zhang group illustrates the conformations of the enamine and aldol acceptor, but ignores conformations of the catalyst.

We recalculated their transition structures at the M06-2X/def2-TZVPP-IEF-PCM//B3LYP-6-31G(d)-IEF-PCM (cyclohexanone) level of theory. The four lowest-energy transition structures are shown in Figure 5. **TS-5a**, **TS-5c**, and **TS-5d** are consistent with the transition structures reported by Zhang. However, we located a new low-energy stereoisomer, **TS-5b**. **TS-5a** leads to the major (*R*,*S*) *anti*-product and is the lowest-energy transition structure. **TS-5b** leads to the (*R*,*R*) *syn*-diastereomer and is higher in energy by 1.5 kcal/mol compared with **TS-5a**, in close agreement with the experimental diastereoselectivity. **TS-5c** leads to the (*S*,*S*) *syn*-diastereomer and is higher in energy by 3.6 kcal/mol. **TS-5d**, which forms the minor (*S*,*R*) stereoisomer, is higher in energy by 4.2 kcal/mol. The energy difference between **TS-5a** and **TS-5d** reproduces the enantioselectivity found by Zhang.

We found that the transition structures again have heavy atoms arranged in conformations resembling those of cyclooctane,[28] and are analogous to the results of the cinchona alkaloid-catalyzed reaction of cyclohexanone and *p*-nitrobenzaldehyde in their relative trend of energies (Figure 1). The lowest-energy transition structure, **TS-5a**, is in the crown conformation. **TS-5b** is also in a crown conformation but has an axial aryl group of the aldehyde. **TS-5c** is in the boat-chair conformation, and is destabilized due to an eclipsed forming C−C bond and steric interactions between the enamine and catalyst. **TS-5d** is in the chair-boat conformation. Both **TS-5a** and **TS-5d** contain staggered chair conformations at the forming C−C bond and have enamines in s-trans conformations. The source of destabilization of **TS-5d** is due to the steric H···H interactions between the axial methylene of cyclohexanone and the catalyst. Shown in Figure 5, the H···H

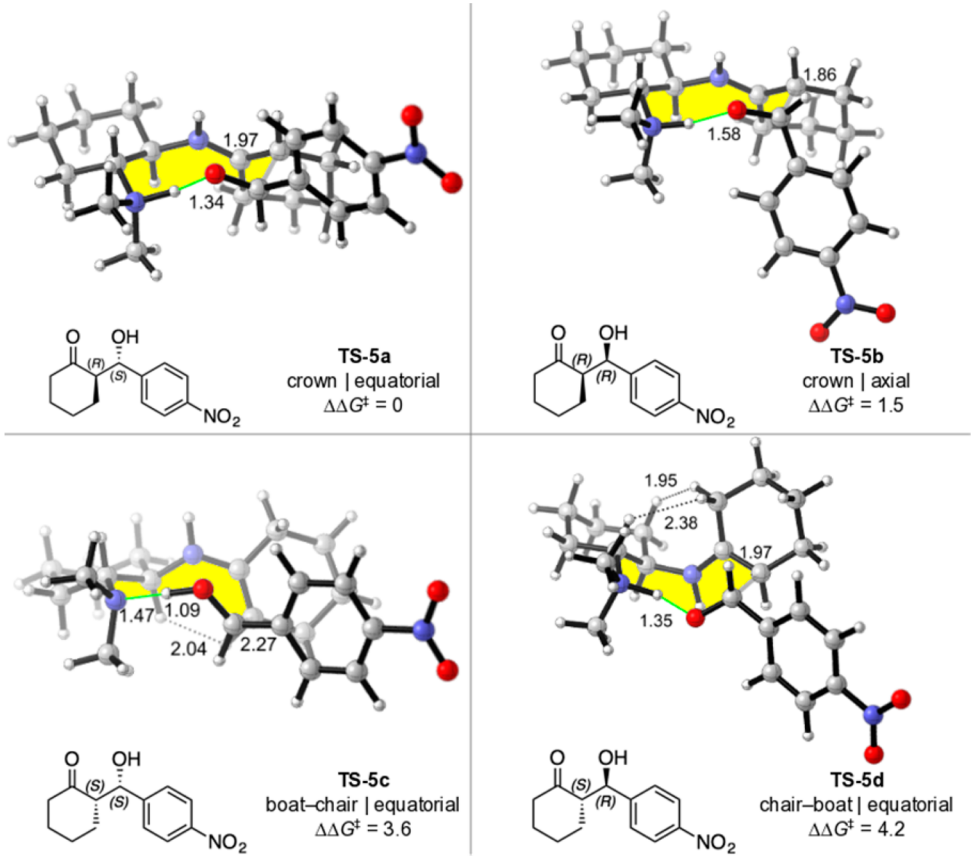

Figure 5. Lowest-energy transition structures **TS-5a−d** for the aldol addition of *p*-nitrobenzaldehyde and the enamine formed by **3** and cyclohexanone (M06-2X/def2-TZVPP-IEF-PCM//B3LYP/6-31G(d)-IEF-PCM (cyclohexanone)). The free energies of activation ($\Delta\Delta G^{\ddagger}$), relative to **TS-5a**, are reported in kcal/mol.

DOI: 10.1021/acs.joc.6b02542
J. Org. Chem. 2016, 81, 12408−12415

distances are 1.95 and 2.38 Å, which are not present in **TS-5a** because the axial methylene is distant from the cyclohexyl portion of the catalyst.

In the studies of Yamamoto's catalyst,[15] we found that the lowest-energy transition structure, i.e., the crown, acquired (+)-gauche conformations about both the forming C−C bond and the NCCN dihedral of the catalyst. In contrast, the higher-energy transition structures were in various combinations of (+)- and (−)-gauche conformations about these two bonds.

The lowest-energy transition structures for the Chimni, Liu, and Luo reactions either have matching (+)- or (−)-gauche conformations at both the forming C−C bonds and NCCN dihedrals. In these systems, the NCCN dihedral of the catalyst is fixed either due to rigidity (1,2-diaminocyclohexane) or conformational preference (cinchona alkaloid-derived primary amines). When the diamine is (+)-gauche, then the major product has a (+)-gauche arrangement about the forming bond. These results are summarized in Scheme 9. The NCCN dihedral of the vicinal diamines is a predictable measure for the gauche conformation about the forming C−C bond in the crown conformation.

Scheme 9. Summary of Results

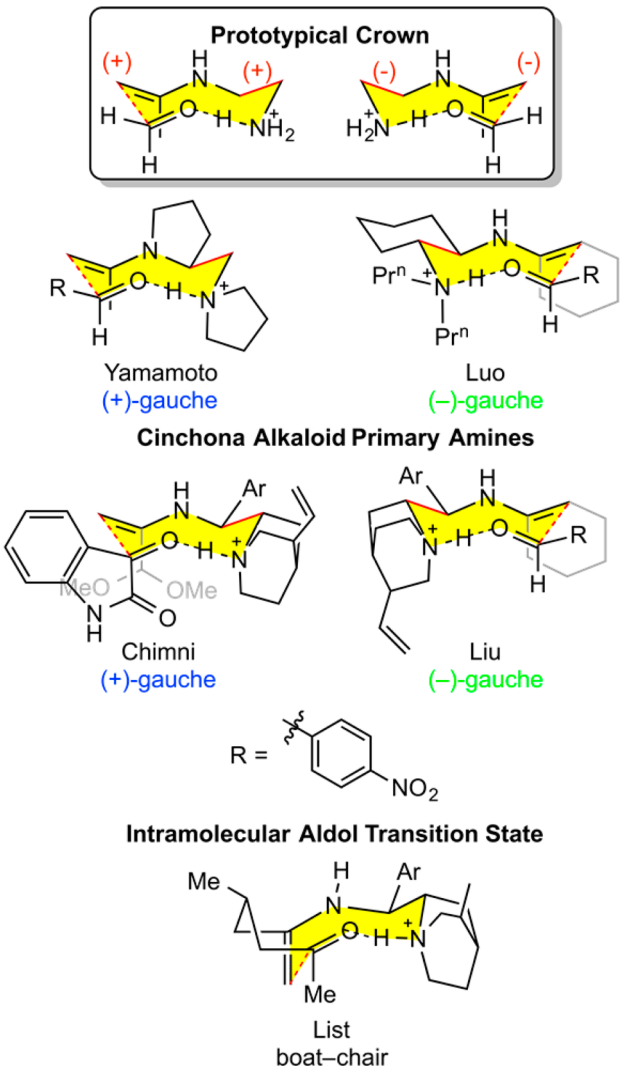

CONCLUSIONS

Cyclic transition structures are preferred for vicinal-diamine catalyzed aldol reactions. The crown conformer is consistently the lowest-energy transition structure in bimolecular systems, unless secondary interactions destabilize the crown or stabilize the chair-boat (e.g., Figure 3). The crown has trans-enamine and staggered chair arrangements of both the forming bond and catalyst. The gauche conformations about the NCCN bond and forming C−C bond of the catalyst are both (+) or (−) for the crown conformations. We have found this to be the case in five examples (Scheme 9). In addition, we have predicted the preferences of the minor enantiomer, being either a chair-boat or crown with an axial substituent depending on the system. Diastereoselectivity relies on the difference in energy between the two crown conformations, analogous to the Zimmerman−Traxler model.[29] In intramolecular aldol reactions, the boat-chair conformation is preferred (Scheme 9).[9a]

The model proposed here explains the source of asymmetric induction for aldol reactions catalyzed by both simple and complex vicinal diamines. The general features of this system have been invoked to explain other vicinal diamine-catalyzed reactions.[30] The predictability and reliability of these mechanistic insights should assist in the rational design of vicinal diamine-catalyzed reactions of aldol, Mannich, and other carbonyl functionalizing reactions.

ASSOCIATED CONTENT

Supporting Information

The Supporting Information is available free of charge on the ACS Publications website at DOI: 10.1021/acs.joc.6b02542.

Complete set of aldol transition structures and their energies for the cinchona alkaloid-derived primary amine-catalyzed aldol reactions, Cartesian coordinates and thermodynamic parameters (in hartrees) of all stationary points (PDF)

AUTHOR INFORMATION

Corresponding Author

*houk@chem.ucla.edu

ORCID

Adam Simon: 0000-0001-6334-3359
Yu-hong Lam: 0000-0002-4946-1487

Notes

The authors declare no competing financial interest.

ACKNOWLEDGMENTS

Financial support was provided by the National Science Foundation (CHE-1361104). A.S. was supported by the NIH Chemistry-Biology Interface Research Training Grant (USPHS National Research Service Award T32GM008496). A.J.Y. is a recipient of the Arnold and Mabel Beckman Foundation undergraduate fellowship. This work used computational and storage services associated with the Hoffman2 Shared Cluster provided by UCLA Institute for Digital Research and Education's (IDRE) Research Technology Group. This work used the Extreme Science and Engineering Discovery Environment (XSEDE), which is supported by National Science Foundation grant number ACI-1053575.

DOI: 10.1021/acs.joc.6b02542
J. Org. Chem. 2016, 81, 12408−12415

REFERENCES

(1) (a) Bertelsen, S.; Jørgensen, K. A. *Chem. Soc. Rev.* **2009**, *38*, 2178−2189. (b) Melchiorre, P.; Marigo, M.; Carlone, A.; Bartoli, G. *Angew. Chem., Int. Ed.* **2008**, *47*, 6138−6171. (c) Mukherjee, S.; Yang, J. W.; Hoffmann, S.; List, B. *Chem. Rev.* **2007**, *107*, 5471−5569. (d) Lelais, G.; MacMillan, D. W. C. *Aldrichimica Acta* **2006**, *39*, 79−87. (e) Melchiorre, P. *Angew. Chem., Int. Ed.* **2012**, *51*, 9748−9770.

(2) (a) List, B.; Lerner, R. A.; Barbas, C. F., III. *J. Am. Chem. Soc.* **2000**, *122*, 2395−2396. (b) List, B. *Tetrahedron* **2002**, *58*, 5573−5590. (c) Movassaghi, M.; Jacobsen, E. N. *Science* **2002**, *298*, 1904−1905.

(3) (a) Bahmanyar, S.; Houk, K. N. *J. Am. Chem. Soc.* **2001**, *123*, 12911−12912. (b) Bahmanyar, S.; Houk, K. N.; Martin, H. J.; List, B. *J. Am. Chem. Soc.* **2003**, *125*, 2475−2479.

(4) (a) Nakadai, M.; Saito, S.; Yamamoto, H. *Tetrahedron* **2002**, *58*, 8167−8177. (b) Saito, S.; Yamamoto, H. *Acc. Chem. Res.* **2004**, *37*, 570−579.

(5) (a) Luo, S.; Xu, H.; Li, J.; Zhang, L. A.; Cheng, J.-P. *J. Am. Chem. Soc.* **2007**, *129*, 3074−3075. (b) Zhang, L.; Fu, N.; Luo, S. *Acc. Chem. Res.* **2015**, *48*, 986−997.

(6) (a) Dijkstra, G. D. H.; Kellogg, R. M.; Wynberg, H.; Svendsen, J. S.; Marko, I.; Sharpless, K. B. *J. Am. Chem. Soc.* **1989**, *111*, 8069−8076. (b) Dijkstra, G. D. H.; Kellogg, R. M.; Wynberg, H. *J. Org. Chem.* **1990**, *55*, 6121−6131. (c) Bürgi, T.; Baiker, A. *J. Am. Chem. Soc.* **1998**, *120*, 12920−12926.

(7) Moran, A.; Hamilton, A.; Bo, C.; Melchiorre, P. *J. Am. Chem. Soc.* **2013**, *135*, 9091−9098.

(8) Olsen, R. A.; Borchardt, D.; Mink, L.; Agarwal, A.; Mueller, L. J.; Zaera, F. *J. Am. Chem. Soc.* **2006**, *128*, 15594−15595.

(9) (a) Lam, Y.-h.; Houk, K. N. *J. Am. Chem. Soc.* **2015**, *137*, 2116−2127. (b) Lam, Y.-h.; Houk, K. N. *J. Am. Chem. Soc.* **2014**, *136*, 9556−9559.

(10) Zheng, B.-L.; Liu, Q.-Z.; Guo, C.-S.; Wang, X.-L.; He, L. *Org. Biomol. Chem.* **2007**, *5*, 2913−2915.

(11) Zhou, J.; Wakchaure, V.; Kraft, P.; List, B. *Angew. Chem., Int. Ed.* **2008**, *47*, 7656−7658.

(12) Guo, Q.; Zhao, J. C.-G. *Tetrahedron Lett.* **2012**, *53*, 1768−1771.

(13) Kumar, A.; Chimni, S. S. *Eur. J. Org. Chem.* **2013**, *2013*, 4780−4786.

(14) McCooey, S. H.; Connon, S. J. *Org. Lett.* **2007**, *9*, 599−602.

(15) Simon, A.; Lam, Y.-h.; Houk, K. N. *J. Am. Chem. Soc.* **2016**, *138*, 503−506.

(16) Sun, X.; Zhu, R.; Gao, J.; Zhang, D.; Feng, D. *J. Phys. Chem. A* **2012**, *116*, 7082−7088.

(17) Frisch, M. J.; Trucks, G. W.; Schlegel, H. B.; Scuseria, G. E.; Robb, M. A.; Cheeseman, J. R.; Scalmani, G.; Barone, V.; Mennucci, B.; Petersson, G. A.; Nakatsuji, H.; Caricato, M.; Li, X.; Hratchian, H. P.; Izmaylov, A. F.; Bloino, J.; Zheng, G.; Sonnenberg, J. L.; Hada, M.; Ehara, M.; Toyota, K.; Fukuda, R.; Hasegawa, J.; Ishida, M.; Nakajima, T.; Honda, Y.; Kitao, O.; Nakai, H.; Vreven, T.; Montgomery, J. A., Jr.; Peralta, J. E.; Ogliaro, F.; Bearpark, M.; Heyd, J. J.; Brothers, E.; Kudin, K. N.; Staroverov, V. N.; Keith, T.; Kobayashi, R.; Normand, J.; Raghavachari, K.; Rendell, A.; Burant, J. C.; Iyengar, S. S.; Tomasi, J.; Cossi, M.; Rega, N.; Millam, J. M.; Klene, M.; Knox, J. E.; Cross, J. B.; Bakken, V.; Adamo, C.; Jaramillo, J.; Gomperts, R.; Stratmann, R. E.; Yazyev, O.; Austin, A. J.; Cammi, R.; Pomelli, C.; Ochterski, J. W.; Martin, R. L.; Morokuma, K.; Zakrzewski, V. G.; Voth, G. A.; Salvador, P.; Dannenberg, J. J.; Dapprich, S.; Daniels, A. D.; Farkas, O.; Foresman, J. B.; Ortiz, J. V.; Cioslowski, J.; Fox, D. J. *Gaussian 09*, Rev. D.01; Gaussian, Inc.: Wallingford, CT, 2013.

(18) (a) Vosko, S. H.; Wilk, L.; Nusair, M. *Can. J. Phys.* **1980**, *58*, 1200−1211. (b) Lee, C.; Yang, W.; Parr, R. G. *Phys. Rev. B: Condens. Matter Mater. Phys.* **1988**, *37*, 785−789. (c) Becke, A. D. *J. Chem. Phys.* **1993**, *98*, 5648−5652. (d) Stephens, P. J.; Devlin, F. J.; Chabalowski, C. F.; Frisch, M. J. *J. Phys. Chem.* **1994**, *98*, 11623−11627.

(19) Tomasi, J.; Mennucci, B.; Cammi, R. *Chem. Rev.* **2005**, *105*, 2999−3094.

(20) (a) Ribeiro, R. F.; Marenich, A. V.; Cramer, C. J.; Truhlar, D. G. *J. Phys. Chem. B* **2011**, *115*, 14556−14562. (b) Zhao, Y.; Truhlar, D. G. *Phys. Chem. Chem. Phys.* **2008**, *10*, 2813−2818.

(21) Zhao, Y.; Truhlar, D. *Theor. Chem. Acc.* **2008**, *120*, 215−241.

(22) Weigend, F.; Ahlrichs, R. *Phys. Chem. Chem. Phys.* **2005**, *7*, 3297−3305.

(23) Simón, L.; Goodman, J. M. *Org. Biomol. Chem.* **2011**, *9*, 689−700.

(24) Banks, J. L.; Beard, H. S.; Cao, Y.; Cho, A. E.; Damm, W.; Farid, R.; Felts, A. K.; Halgren, T. A.; Mainz, D. T.; Maple, J. R.; Murphy, R.; Philipp, D. M.; Repasky, M. P.; Zhang, L. Y.; Berne, B. J.; Friesner, R. A.; Gallicchio, E.; Levy, R. M. *J. Comput. Chem.* **2005**, *26*, 1752−1780.

(25) *Schrödinger Release 2015−3: MacroModel*, version 10.9; Schrödinger, LLC: New York, NY, 2015.

(26) Legault, C. Y. *CYLview*, 1.0b; Université de Sherbrooke, 2009; http://www.cylview.org.

(27) Lam, Y.-h.; Grayson, M. N.; Holland, M. C.; Simon, A.; Houk, K. N. *Acc. Chem. Res.* **2016**, *49*, 750−762.

(28) Wiberg, K. B. *J. Org. Chem.* **2003**, *68*, 9322−9329.

(29) Zimmerman, H. E.; Traxler, M. D. *J. Am. Chem. Soc.* **1957**, *79*, 1920−1923.

(30) Mose, R.; Jensen, M. E.; Preegel, G.; Jørgensen, K. A. *Angew. Chem., Int. Ed.* **2015**, *54*, 13630−13634.

DOI: 10.1021/acs.joc.6b02542
J. Org. Chem. 2016, 81, 12408−12415